SIMULATION OF OIL–WATER FLOW WITH PERMEABILITY VARIATION DUE TO INCOMPATIBLE BRINE SALINITIES

Adnan E. Omar

Petroleum Engineering Department
King Saud University, P.O. Box 800
Riyadh, 11421 Saudi Arabia

الخلاصـــة :

تم تطوير محاكي عددي لطوريْن في بُعد واحد لنموذج سريان الزيت والماء، وهذا المحاكى يأخذ في الاعتبار الفرق في الملوحة بين المحلول المشبع والمحلول المزيح، ويشمل النموذج الرياضي لهذه الظواهر معادلات سريان الزيت والماء مقترنة بمعادلة الحمل والانتشار والتي تصف حركة الملح في الوسط المائي. وقد استُعملت طريقة حلّ الفروق المحدودة لحساب الضغوط ودرجات التشبع وذلك بمعلومية درجة ملوحة الماء المزيح، وبعض خواص الصخر والتي تم قياسها معمليا.

ولقد تم استعمال حسابات النموذج الرياضي لمحاكاة عدة تجارب إزاحة. وكان التنبؤ بانخفاض الضغط عبر العينات الصخرية دقيقا عند مقارنته بانخفاض الضغط عبر العينات والمقاس معمليا اذ كان أقصى خطأ هو ١,٣٩٪. وهذا الخطأ الأقصى المئوي ازداد الى ١٥,٣٪ عند مقارنة النفاذية النسبية المحسوبة باستعمال المحاكي مع تلك التي حسبت من النتائج المعملية باستعمال طريقة (جونسون وزميله JBN). وهذه الزيادة في الخطأ الأقصى المئوي ترجع الى أن طريقة (جونسون وزميله JBN) لا تعطى نتائج دقيقة عندما لا تتوافق ظروف السريان مع افتراضات نظرية (بكلي وليفريت).

ABSTRACT

A numerical simulator (two phase, one dimensional, oil–water fluid flow model) was developed which takes into consideration the difference between the salinities of the injected and saturating brines. The mathematical model encompassing the above phenomena was formulated from oil–water flow equations coupled with the convective–diffusive equation which describes the movement of salt in the aqueous phase. A finite difference solution was applied to compute pressures and saturations given the injected water salinity and a few rock parameters determined by laboratory experiments.

The mathematical model calculations were carried out to simulate laboratory displacement runs. The predicted pressure drop was accurate when compared to the experimental pressure drop across the cores with a maximum error of 1.39%. This error, however, increases to 15.30% when the computed relative permeabilities were compared to those calculated from experimental data using the JBN method. This was attributed to inaccuracies inherent to the JBN method when flow conditions do not satisfy Buckley–Leverett theory assumptions.

Adnan E. Omar

SIMULATION OF OIL–WATER FLOW WITH PERMEABILITY VARIATION DUE TO INCOMPATIBLE BRINE SALINITIES

NOMENCLATURE

A	bulk cross-sectional area
C	concentration
E	absolute percentage error
k	permeability
K	dispersion coefficient, (area/time)
L	length
m^*	salt production rate
P	pressure
q	volumetric flow rate
S	saturation
T	transmissibility
t	time
V_b	volume of grid block
V_w	aqueous phase velocity

Greek

β	formation volume factor (volume/volume)
ϕ	porosity
Φ	potential
μ	viscosity
σ^2	standard deviation

Subscripts

av	average
i	initial condition
iw	irreducible water
o	oil
or	residual oil
r	residual
ro	relative to oil
rw	relative to water
w	water

INTRODUCTION

Many methods are available for the prediction of water flooding performance, and in order to analyze the data compiled during a water flooding experiment a steady state or an external drive method will be sought. Steady state methods only apply to experiments when no saturation gradient exists. Such experiments are cumbersome and time consuming. On the other hand most external drive methods are limited to displacements in which the assumptions underlying the Buckley–Leverett theory are met [1]; of these the JBN [2] and the Jones and Rozelle [3] methods are the most widely used. In special cases, when the properties of the fluids and their mobility ratios change, the saturation profiles are no longer monotonic and the Buckley and Leverett assumptions are no longer satisfied.

One of these cases arises when simulating waterflooding operations in Saudi fields. Saudi oil fields connate brines are characterized by a high salt concentration (25 wt. % typically, and could reach 30 wt. %). Seawater is used in water flooding operations; therefore the properties of the connate and displacing waters are at variance. The difference in the properties of the connate and injected waters leads to different mobility ratios at the displacement front as the salts disperse between the connate and displacing brine.

In this work a numerical simulator (a single dimension two phase oil–water flow model) is presented to account for the variation in the properties and the relative mobility of the water phase, due to the dispersion of the salt between the connate and displacing brines. The oil–water flow equations were coupled weakly with the convective–diffusive equation which describes the movement of the salt within the aqueous phase. The finite difference method was used to compute the pressures and saturations from the injected water salinity and a few rock and fluids parameters.

Experimental work was conducted with long thin Berea sandstone cores and the pressure drop across the cores was compared to the computer model output. The water flooding data were then analyzed and the resulting relative permeabilities were compared to the relative permeabilities, computed from the saturations predicted by the model using published correlations [4].

THE MODEL

The mathematical model was formulated for the single dimension case of two phase flow through porous media with permeability variation due to salt dispersion between the injected and saturating brines. The two phase flow equations were formulated with permeability expressed as a function of saturation. A separate convective diffusive equation which describes the movement of salt in aqueous phase was

also developed. This equation allows for local aqueous phase saturations. The two phase oil–water equation and the convective–diffusive equation were coupled with introduced allowance for the variation of fluids properties.

Basic Assumptions and Program Input

The basic assumptions for applying this model numerically are that the flow is in two phases, single dimension, the effect of gravity is neglected, the fluids are incompressible, the aqueous phase may consist of two components: water and salt, oleic phase consists of only a single component, relative permeability is a function of the saturation, and temperature is constant at standard level 15.6°C (60°F).

The governing equations are:

$$\frac{\partial}{\partial x}\left(\frac{kk_{ro}}{\mu_o\beta_o}\frac{\partial P_o}{\partial x}\right) + \frac{q_o^*}{V_b} = \phi\frac{\partial}{\partial t}\left(\frac{S_o}{\beta_o}\right) \qquad (1)$$

$$\frac{\partial}{\partial x}\left(\frac{kk_{rw}}{\mu_w\mu_w}\frac{\partial P_w}{\partial x}\right) + \frac{q_w^*}{V_b} = \phi\frac{\partial}{\partial t}\left(\frac{S_w}{\beta_w}\right) \qquad (2)$$

where, $\beta_o = \beta_w = 1$

$$\frac{\partial}{\partial x}\left(K_\ell\frac{\partial C}{\partial x}\right) - V_w\frac{\partial C}{\partial x} + m^* = (\phi S_w)\frac{\partial C}{\partial t} \qquad (3)$$

The finite difference formulation for the above equations is in Appendix A.

EXPERIMENTAL WORK

The experimental work consisted of flooding Berea core samples, already containing both oil and highly saline water similar to Saudi oil field connate water, with solutions of sodium chloride ranging in concentration from 0.6 to 15.0 wt. %. The relative permeabilities were calculated using the JBN method [2] (Appendix B).

1. Core Samples

Berea sandstones were used exclusively for two reasons: (1) the variation of Saudi mineralogy makes it very hard to relate the results obtained from a given set of cores to another or to make any generalizations; (2) Berea sandstone has acquired a reference position in petrophysical experiments because of their homogeneity and water sensitivity. Core samples of 1.22 m (4 feet) length were used. The physical properties of the core samples are listed in Table 1.

Table 1. Physical Properties of Four Feet Berea Sandstone Cores.

Core No.	Diameter (cm)	Length (cm)	Porosity %	S_{iw}%	Initial Permeability
B1	5.11	121.92	22.56	28.0	338.4
B2	5.11	121.92	25.96	31.2	300.6
B3	5.11	121.92	23.39	28.7	305.5
B4	5.11	121.92	26.60	29.5	326.6

The cores were not fired or pretreated, and nothing was done to neutralize the clay present in them. A minimum injected salt concentration of 0.6 wt. % sodium chloride was chosen to avoid the effects of clay swelling and the migration of clay particles in the cores. The dimensions of the cores were chosen to reduce the effect of lateral flow and gravity.

2. Brine

The cores were initially saturated with formation brine obtained from Saudi oil fields (Table 2). The concentrations of the displacing brines were 15, 10, 5, and 0.6 wt. % NaCl. The viscosity and the density of the displaced and the displacing brines were determined (Tables 3 and 4). The viscosity as a function of concentration was obtained from Reference [5]. The density was obtained from Reference [6]. All brines were prefiltered and treated to avoid bacterial plugging.

3. Oil

The oil used in the two phase flow experiments was a Saudi crude oil from Safaniya. The properties of this crude oil were obtained from Reference [6] (Table 3).

LABORATORY EQUIPMENT

Figure 1 is a schematic diagram of the equipment used. It consists of fluid reservoirs feeding to a non-pulsating, constant rate pump capable of delivering constant rates ranging from 0.9 cc/h to 640 cc/h. The fluids delivered by the pump pass through a filter block before entering the core sample. After being filtered, the fluids are directed to the four feet core assembly. The effluent fluids from the core samples are collected by a fractional collector. Pressure gauges are mounted at the inlet ends of the core.

Table 2. Formation Water Analysis.

Ions	Milligrams per litre (mg/l)	Equivalent weight (eq. wt.)	Milli-equivalent/litre (meq/l)	% Reacting value
A – Positive Radicals				
1. Alkali				
Sodium, Na^+	67 000.0	23.000	2913.04	36.150
Potassium, K^+	0.0	39.102	0.00	0.000
2. Alkaline earth				
Calcium, Ca^{+2}	18 600.0	20.040	928.040	11.518
Magnesium, Mg^{+2}	2 270.0	12.560	186.74	2.317
Barium, Ba^{+2}	0.0	68.670	0.00	0.000
Strontium, Sr^{+2}	0.0	43.810	0.00	0.000
3. Metals				
Aluminium, Al^{+3}	0.0	8.733	0.00	0.000
Iron, Fe^{+3}	0.0	18.616	0.00	0.000
Manganese, Mn^{+3}	0.0	27.469	0.00	0.000
B – Negative Radicals				
1. Strong acid				
Chloride, Cl^-	142 500.0	35.453	4019.41	49.879
Sulphate, SO_4^{-2}	260.0	48.032	5.41	0.067
2. Weak acid				
Bicarbonate, HCO_3^-	340.0	61.000	5.57	0.069
Carbonate, CO_3^{-2}	0.0	30.000	0.00	0.000
Sulphide, S^{-2}	0.0	16.032	0.00	0.000
Total	230 970.0		8085.31	100.000

Table 3. Physical Properties of Formation Water and the Oil Used.

	Formation Water	Oil
Surface Tension, dyne cm^{-1}	555.3	28.8
Density, g cm^{-3}	1.1605	0.9204
Viscosity, cp	1.80	21.65

Table 4. Physical Properties of the Injected Brines.

Concentration % wt. Nacl	Density g cm^{-3}	Viscosity cp	Surface Tension dyne cm^{-1}
0.6	1.0025	1.011	50.65
5.00	1.0340	1.083	51.62
10.00	1.0707	1.191	52.80
15.00	1.1085	1.349	53.92

PROCEDURE

The Berea core samples were initially saturated with brine obtained from a Saudi oil field, Table 2. Then the cores were flooded with the Safaniya crude oil until irreducible water saturations were established, Table 1. Different brines (Table 5) were used

Table 5. Experimental Runs on Berea Sandstone Cores Saturated with Formation Water and Oil.

Core No.	Displacing Brine Concentration (% wt. Bacl)
B1	15
B2	10
B3	5
B4	0.6

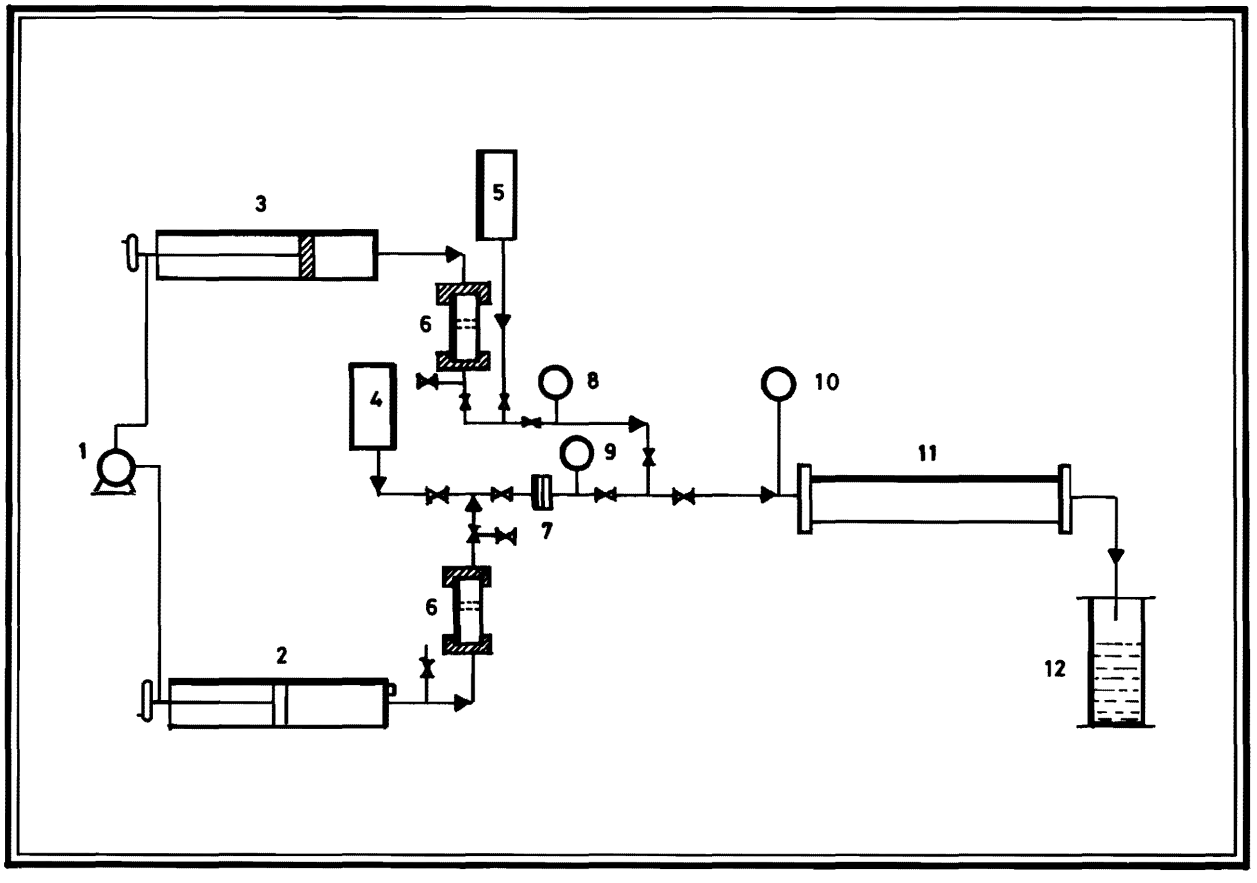

1. Pump drive
2. Pump brine reservoir and piston
3. Pump oil reservoir and piston
4. Brine reservoir
5. Oil reservoir
6. Floating piston cylinder
7. Brine filter
8. Oil pressure gauge
9. Brine pressure gauge
10. Upstream pressure gauge
11. Core holder [4 foot]
12. Measuring cylinder

Figure 1. Schematic Diagram of Experimental Fluid Flow Equipment.

to displace fluids to determine the relative permeabilities to oil and water using the JBN method described in Appendix B. The experimental data from the displacements are listed in Appendix C.

RESULTS AND DISCUSSIONS

Two sets of data were obtained: the first set was obtained from the experimental work; experimental data (Appendix C) were analysed using the JBN method (Appendix B) which resulted in obtaining terminal saturations and relative permeability curves (Figure 2). The other set of data were obtained by computer simulation using the basic rock and fluid properties and irreducible brines saturations with the density of the brine and its viscosity treated as functions of the concentration of the brine. The total pressure drop and saturations were computed at time intervals to compare them with the experimental results. Relative permeabilities as functions of local saturation of the cores were calculated from published correlations (Equations 22 & 23) [7]. The resulting relative permeability curves using terminal saturations are given in Figure 2.

Pressure Drop Data Analysis

Table 6 shows the variation of the standard deviation and the average absolute percentage error of predicted pressure drop from the experimental pressure drop. The values of both statistical parameters are very low (the maximum average percentage error being 1.39%), reflecting a very accurate algorithm. This low deviation and average error also reflects ex-

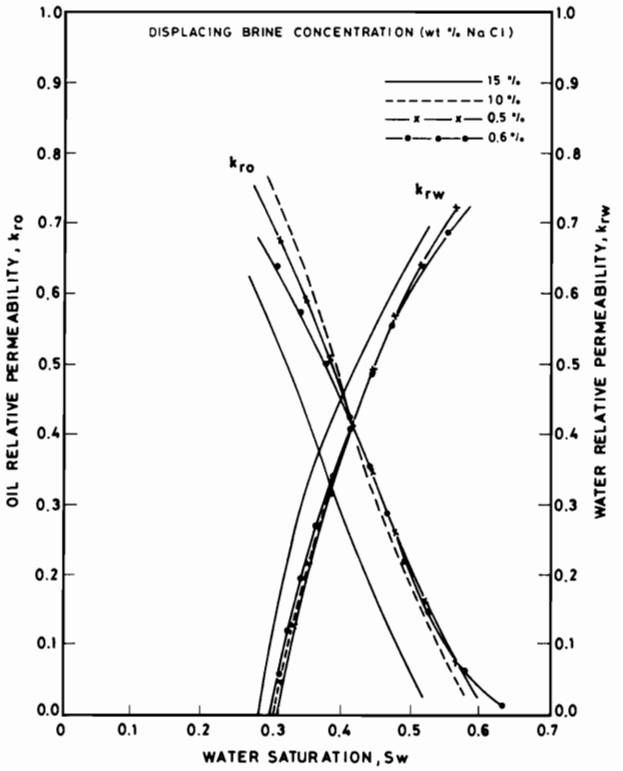

Figure 2. Effect of Displacing Brine Concentration on Relative Permeability, Temperature 15.6°C.

Table 6. Standard deviation (σ^2) and Absolute percentage error (E) of Computed Pressure Drop from Experimental Pressure Drop.

Core No.	ΔP σ^2	ΔP E
1	6.87	1.39
2	4.36	1.17
3	5.23	1.24
4	5.91	1.09

perimental conditions complying with the theoretical assumption which form the bases of the model, namely the absence of an appreciable lateral movement, no gravity effects, and the absence of any end effects.

Relative Permeability Data Analysis

Table 7 shows the variation of the average standard deviation and the average percentage error of the predicted relative permeabilities at the different

Table 7. Average Standard Deviation (σ^2) and Absolute Percentage Error (E) of Computed Relative Permeabilities With Calculated Relative Permeabilities Using JBN Method.

Core No.	k_{ro} σ^2	k_{rw} σ^2	k_{ro} E	k_{rw} E
1	0.13165	0.16551	15.30	14.89
2	0.112598	0.16702	12.16	12.04
3	0.12866	0.15183	11.57	10.19
4	0.11940	0.12007	8.62	8.83

salinities from the experimental data. Ironically, the average percentage error is no longer low (15.30% maximum) and is noticeably higher than in the case of the pressure drop data analysis. If the accuracy of the relative permeability correlations (Equations 1 & 2) was not doubted (see Reference [5]) then the failure of the JBN method to predict accurate relative permeability data is clearly established. Another observed factor that supports this conclusion is the fact that the absolute value of the average percentage error increased sharply with the increase in the difference between the salinity of the injected and saturating brines. This, not an unexpected fact, is explained by a change of up to 88% in the local mobility ratio which is not accounted for when using the JBN method. One could have expected an even higher percentage error, but the JBN procedure includes two numerical differentiations which tend to smooth the final curves, and since the same residual saturations were used by the two sets of data then this tends to reduce the average percentage error and the standard deviation. One should also point out to the fact that when sharp variations in local mobility ratios occur within the core, the Buckley–Leverett theorem assumptions do no longer hold. Hence the analysis of the displacement data using the JBN method leads to inaccurate results.

CONCLUSION

The adequacy of the developed simulator was established from the comparison of the computed pressure drop with the experimental pressure drop. The resulting data were accurate when compared to experimental data (maximum error was 1.39%). Relative permeability data computed from the simulation results did not show the same correspondence when compared with the same data calculated from the experimental work using JBN method (an increase in

the maximum percentage error of up to 15.30%). This was attributed to the fact that the Buckley–Leverett theory assumptions do not apply in this case and consequently the application of the corresponding numerical methods such as the JBN will lead to inaccurate results in this particular case where appreciable changes in the mobility ratio within the cores occur. The model simulates displacement tests efficiently in the case of incompatible injected and saturating brine, a case which occurs frequently in Saudi Arabian fields. The model can thus be incorporated in any water flood pilot mathematical simulator under these conditions.

REFERENCES

[1] S.E. Buckley and M.C. Leverett, "Mechanism of Fluid Displacement in Sands", *Trans. AIME*, **146** (1942), p. 107.

[2] E.F. Johnson, D.P. Bossler, and V.O. Neumann, "Calculation of Relative Permeability from Displacement Experiments", *Trans. AIME*, **216** (1959), p. 370.

[3] S.C. Jones and W.O. Roszelle, "Graphical Techniques for Determining Relative Permeability from Displacement Experiments", *J. Pet. Technol.*, May, 1978, p. 807.

[4] *Handbook of Chemistry and Physics*, 26th Edn, Boca Raton: CRC Press, 1976.

[5] A.E. Omar, M.M. El-Gassier, and A.S. Dahab, "Effect of Salinity on Permeability", *Final Report KACST Project AR-5-28*, 1988.

[6] A.M. Totonji, *et al*, "Enhanced Oil Recovery of Saudi Oil Fields by Surfactant Polymer Flooding", *KACST Project AR-3-012 Final Report*, p. 126.

[7] H.J. Welge, "Simplified Method for Computing Oil Recovery by Gas or Water Drives", *Trans. AIME*, **195** (1952), p. 91.

[8] C.S. Land, "Calculation of Imbibition Relative Permeability for Two and Three Phase Flow from Rock Properties", *SPE-1942*, June 1968.

Paper Received 19 November 1989: Revised 14 March 1990, 12 May 1990.

APPENDIX A

Given a grid of N blocks covering a physical length of L and bulk cross-sectional area A, we can write Equations (1)–(3) finite difference form as follows, for some block i:

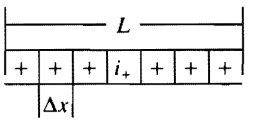

Cross sectional area A.

(a) Oil

$$\frac{kk_{ro}}{\mu(\Delta x)^2}\Bigg|_{i+\frac{1}{2}}^{n+1}(P_{o_{i+1}}^{n+1}-P_{o_i}^{n+1})-\frac{kk_{ro}}{\mu_o(\Delta x)^2}\Bigg|_{i-\frac{1}{2}}^{n+1}$$

$$\times(P_{o_i}^{n+1}-P_{o_{i-1}}^{n+1})+\frac{q_{o_i}^*}{V_{b_i}}=\phi\frac{S_{o_i}^{n+1}-S_{o_i}^{n}}{\Delta t} \tag{4}$$

(b) Water

$$\frac{kk_{rw}}{\mu_w(\Delta x)^2}\Bigg|_{i+\frac{1}{2}}^{n+1}(P_{w_{i+1}}^{n+1}-P_{w_i}^{n+1})-\frac{kk_{rw}}{\mu_w(\Delta x)^2}\Bigg|_{i-\frac{1}{2}}^{n+1}$$

$$\times(P_{w_i}^{n+1}-P_{w_{i-1}}^{n+1})+\frac{q_{w_i}^*}{V_{b_i}}=\phi\frac{S_{w_i}^{n+1}-S_{w_i}^{n}}{\Delta t} \tag{5}$$

(c) Salt Concentration

$$\frac{1}{(\Delta x)^2}\left[K_{\ell_{i+\frac{1}{2}}}^{n}(C_{i+1}^{n+1}-C_i^{n+1})-K_{\ell_{i-\frac{1}{2}}}^{n}(C_i^{n+1}-C_{i-1}^{n+1})\right]$$

$$-V_w\Bigg|_i^n\frac{C_{i+1}^{n+1}-C_{i-1}^{n+1}}{2(\Delta x)}+m_i^*$$

$$=(\phi S_w^{n+1})_i\frac{C_i^{n+1}-C_i^{n}}{\Delta t} \tag{6}$$

Simplify Equations (4) and (5) as follows: Define transmissibility as

$$T=\frac{Akk_r}{\mu\Delta x}$$

and noting that

$$S_o+S_w=1.0$$

Equations (4) and (5) when added gives:

$$T_{o_{i+\frac{1}{2}}}^{n+1}(P_{o_{i+1}}^{n+1}-P_{o_i}^{n+1})-T_{o_{i-\frac{1}{2}}}^{n+1}(P_{o_i}^{n+1}-P_{o_{i-1}}^{n+1})$$

$$+q_{o_i}^*+q_{w_i}^*+T_{w_{i+\frac{1}{2}}}^{n+1}(P_{w_{i+1}}^{n+1}-P_{w_i}^{n+1})$$

$$-T_{w_{i-\frac{1}{2}}}^{n+1}(P_{w_i}^{n+1}-P_{w_{i-1}}^{n+1})=0 \tag{7}$$

Equation (7) is essentially an equation in pressure only. We shall reduce P_o to P_w, using the capillary pressure equation:

$$P_o=P_w+P_{cow}(S_w) \tag{8}$$

Then Equation (7) becomes

$$-(T_{o_{i-\frac{1}{2}}}^{n+1}+T_{w_{i-\frac{1}{2}}}^{n+1})P_{w_{i-1}}^{n+1}+(T_{o_{i-\frac{1}{2}}}^{n+1}+T_{w_{i-\frac{1}{2}}}^{n+1}+T_{o_{i+\frac{1}{2}}}^{n+1}+$$

$$+T_{w_{i+\frac{1}{2}}}^{n+1})P_{w_i}^{n+1}-(T_{o_{i+\frac{1}{2}}}^{n+1}+T_{w_{i+\frac{1}{2}}}^{n+1})P_{w_{i+1}}^{n+1}=q_{o_i}^*+q_{w_i}^*$$

$$+T_{o_{i+\frac{1}{2}}}^{n+1}(P_{cow_{i+1}}^{n+1}-P_{cow_i}^{n+1})-T_{o_{i-\frac{1}{2}}}^{n+1}(P_{cow_i}^{n+1}-P_{cow_{i-1}}^{n+1}). \tag{9}$$

Equation (9) can be written in the form

$$a_iP_{w_{i-1}}^{n+1}+b_iP_{w_i}^{n+1}+c_iP_{w_{i+1}}^{n+1}=d_i, \tag{10}$$

where

$$\begin{aligned}
a_i &= -(T_{o_{i-\frac{1}{2}}}^{n+1}+T_{w_{i-\frac{1}{2}}}^{n+1})\\
b_i &= T_{o_{i-\frac{1}{2}}}^{n+1}+T_{w_{i-\frac{1}{2}}}^{n+1}+T_{o_{i+\frac{1}{2}}}^{n+1}+T_{w_{i+\frac{1}{2}}}^{n+1}\\
c_i &= -(T_{o_{i+\frac{1}{2}}}^{n+1}+T_{w_{i+\frac{1}{2}}}^{n+1})\\
d_i &= q_{o_i}^*+q_{w_i}^*+T_{o_{i+\frac{1}{2}}}^{n+1}(P_{cow_{i+1}}^{n+1}-P_{cow_i}^{n+1})\\
&\quad -T_{o_{i-\frac{1}{2}}}^{n+1}(P_{cow_i}^{n+1}-P_{cow_{i-1}}^{n+1}).
\end{aligned} \tag{11}$$

Once we have solved for pressure P_w^{n+1}, we can solve for S_o^{n+1} or S_w^{n+1}. From Equation (5) we can solve for $S_{w_i}^{n+1}$

$$\begin{aligned}
S_{w_i}^{n+1} &= S_{w_i}^{n}+\frac{\Delta t}{\phi V_{b_i}}[T_{w_{i+\frac{1}{2}}}^{n+1}(P_{w_{i+1}}^{n+1}-P_{w_i}^{n+1})\\
&\quad -T_{w_{i-\frac{1}{2}}}^{n+1}(P_{w_i}^{n+1}-P_{w_{i-1}}^{n+1})-q_{w_i}^*]
\end{aligned} \tag{12}$$

where, $V_{b_i}=A\Delta x_i$.

Now consider Equation (6), which is solved for salt concentration C^{n+1}. Rearranging:

$$-\left(\frac{K_{\ell_{i-\frac{1}{2}}}^{n}}{(\Delta x)^2}+\frac{V_{w_i}^{n}}{2\Delta x}\right)C_{i+1}^{n+1}+\left(\frac{K_{\ell_{i-\frac{1}{2}}}^{n}}{(\Delta x)^2}+\frac{K_{\ell_{i+\frac{1}{2}}}^{n}}{(\Delta x)^2}\right.$$

$$\left.+\frac{\phi S_{w_i}^{n+1}}{\Delta t}\right)C_i^{n+1}-\left(\frac{K_{\ell_{i+\frac{1}{2}}}^{n}}{(\Delta x)^2}+\frac{V_{w_i}^{n}}{2\Delta x}\right)C_{i+1}^{n+1}=m_i^*$$

$$+\frac{\phi S_{w_i}^{n+1}}{\Delta t} C_i^n. \tag{13}$$

This equation can be written as

$$a_i C_{i-1}^{n+1} + b_i C_i^{n+1} + c_i C_i^{n+1} = d_i \tag{14}$$

where,

$$a_i = -\left(\frac{K_{\ell_{i-\frac{1}{2}}}^n}{(\Delta x)^2} + \frac{V_{w_i}^n}{2\Delta x}\right)$$

$$b_i = \frac{K_{\ell_{i-\frac{1}{2}}}^n}{(\Delta x)^2} + \frac{K_{\ell_{i+\frac{1}{2}}}^n}{(\Delta x)^2} + \frac{\phi S_{w_i}^{n+1}}{\Delta t}$$

$$c_i = -\left(\frac{K_{\ell_{i+\frac{1}{2}}}^n}{(\Delta x)^2} - \frac{V_{w_i}^n}{2\Delta x}\right)$$

$$d_i = m_i^* + \frac{\phi S_{w_i}^{n+1}}{\Delta t} C_i^n \tag{15}$$

The aqueous phase velocity V_{w_i} can be calculated from the following equation for all blocks

$$V_{w_i} = 5.615 \frac{k k_{rw}}{\mu_w}\Bigg|_i^{n+1} \frac{P_{w_{i+1}}^{n+1} - P_{w_{i-1}}^{n+1}}{2\Delta x} \tag{16}$$

The transmissibilities are defined in terms of the properties of adjacent blocks as follow:

$$T_{o_{i+\frac{1}{2}}}^{n+1} = \frac{2A_i A_{i+1} k_i^{n+1} k_{i+1}^{n+1}}{A_i k_i^{n+1} \Delta x_{i+1} + A_{i+1} k_{i+1}^{n+1} \Delta x_i} \times \frac{k_{ro_{i \text{ or } i+1}}^{n+1}}{\frac{1}{2}(M_{o_i}^{n+1} + M_{o_{i+1}}^{n+1})} \tag{17}$$

The right hand side of the above equation is an average value of transmissibilities based on values at the centers of adjacent blocks. Considering $x_{i+1} = x_i = x$ = constant, and that the areas are equal $A_{i+1} = A_i = A$ = constant, hence

$$T_{o_{i+\frac{1}{2}}}^{n+1} = \frac{2k_i^{n+1} k_{i+1}^{n+1} A}{\Delta x (k_i^{n+1} + k_{i+1}^{n+1})} \cdot \frac{k_{ro_{i+1}}^{n+1}}{\frac{1}{2}(M_{o_i}^{n+1} + M_{o_{i+1}}^{n+1})} \tag{18}$$

and

$$T_{o_{i-\frac{1}{2}}}^{n+1} = \frac{2k_i^{n+1} k_{i-1}^{n+1} A}{\Delta x (k_i^{n+1} + k_{i-1}^{n+1})} \frac{k_{ro_i}^{n+1}}{\frac{1}{2}(M_{o_i}^{n+1} + M_{o_{i-1}}^{n+1})} \tag{19}$$

The capillary pressure between oil and water is a function of water saturation. Thus

$$P_{cow} = P_{cow}(S_w). \tag{20}$$

Knowing the function we can easily calculate P_{cow} for any given S_w. For similar oil and brine the following empirical correlation is reported [5]:

$$P_{cow} = 0.8/(S_w)^{0.5} \tag{21}$$

Relative permeabilities to oil and water may be determined as functions of saturations from the following equations [7]:

$$k_{rw} = 1.5814\left(\frac{S_w - S_{iw}}{1 - S_{iw}}\right)^{1.91} - 0.58617\left(\frac{S_w - S_{or}}{1 - S_{iw} - S_{or}}\right) \times (S_w - S_{iw}) - 1.2484(1 - S_{iw})(S_w - S_{iw}) \tag{22}$$

and

$$k_{ro} = 0.76067\left(\frac{1 - S_w}{\frac{1 - S_{iw}}{1 - S_{or}} - S_{or}}\right)^{1.8} + \left(\frac{1 - S_w - S_{or}}{1 - S_{iw} - S_{or}}\right) + 2.6318(1 - S_{or})(1 - S_w - S_{or}) \tag{23}$$

Assume that the boundaries of the flow system are closed by assuming T and K_ℓ values to be equal to zero at the boundaries. The sources terms at the initial blocks where only water is injected at a given rate are $+q_{wi}^*$ and q_{ol}^* (equal zero). At the last block N, both oil and water are produced at rate $-q_{on}^*$ and $-q_{wn}^*$. These rates can be calculated as follows:

$$q_{on}^* + q_{wn}^* = q_{wl}^* \tag{24}$$

and

$$\frac{q_{wn}^*}{q_{on}^*} = \frac{k_{rw} M_o}{\mu_w k_{ro}}\Bigg|_n \tag{25}$$

At block 1 brine is injected with concentration C_o mg/l at a rate of q_{w1}^* *B/D*. Thus:

$$m_1^* = \frac{C_o q_{wl}^* (5.615)}{A \Delta x} \text{ mg l}^{-1}\text{d}^{-1} \tag{26}$$

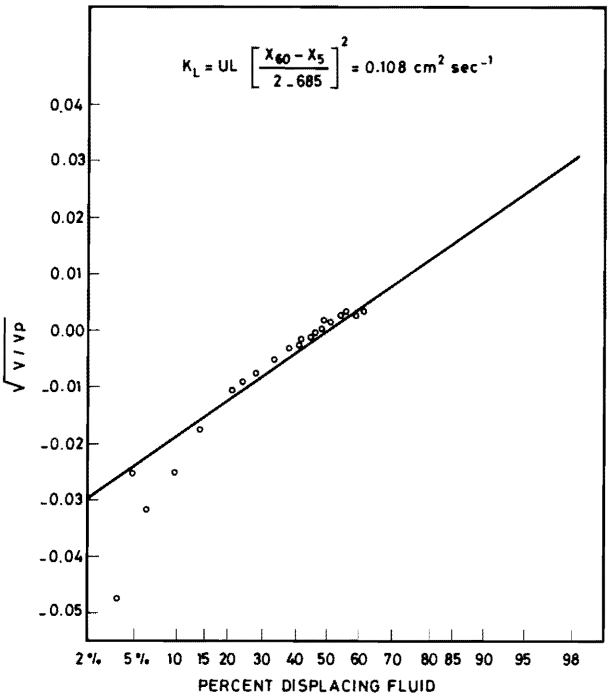

Figure 3. Dispersion Coefficient Determination.

The value of m^* at the outlet end, *i.e.* m_n^* is given by

$$m_n^* = \frac{C_{n-\frac{1}{2}} q_{wn}^* (5.615)}{A \Delta x} \text{ mg l}^{-1}\text{d}^{-1} \qquad (27)$$

The dispersion coefficient can be calculated from our laboratory data as a function of the aqueous phase velocity, pore volume, length of core, and viscosity of aqueous phase.

The dispersion coefficient K_ℓ is calculated from Figure 3 and found to be equal to 0.108 cm^2s^{-1}. This value is used throughout our calculation. However, in the mathematical model we provided for an average dispersion coefficient which was calculated as follows:

$$K_{i\pm\frac{1}{2}} = K_{\ell i} + K_{\ell i\pm 1}. \qquad (28)$$

APPENDIX B CALCULATION OF RELATIVE PERMEABILITIES USING THE JOHNSON–BISSLER–NEUMANN METHOD

This method depends essentially on Welge [8] equations as formulated and expanded by Johnson *et al.* [3]. It requires the knowledge of the porosity and the pore volume (PV), both the viscosities of oil and water, the initial water saturation, the number of pore volumes injected (N_{pv}) at the given time interval, and the water–oil ratio in effluent (WOR). The fraction of displaced phase in the effluent (f_o) would then be defined as:

$$f_o = \frac{1}{1 + WOR}. \qquad (1)$$

If for a certain given reading of oil volume displaced (V_o), the total cumulative oil volume displaced was V_{oc}, then the average water saturation ($S_{w(av)}$) would be defined by the following equation:

$$S_{w(av)} = (V_{oc} - 0.5V_o) / PV + S_w \qquad (2)$$

and hence the water saturation S_w would be equal to:

$$S_w = S_{w(av)} - f_o\left(N_{pv} - \frac{V}{2PV}\right) \qquad (3)$$

where V is the volume of effluent.

The oil saturation S_o would then be:

$$S_o = 1 - S_w \qquad (4)$$

If we define the relative injectivity (I_r) as the ratio of the intake capacity to the initial intake capacity then:

$$I_r = \frac{\dfrac{V}{\Delta t \Delta p}}{\dfrac{V_i}{\Delta t_i \Delta p_i}} \qquad (5)$$

where the subscript i denotes initial conditions when oil alone was flowing through the system. Omitting the lengthy derivations of Welge and Johnson *et al.*, we have:

$$k_{ro} = \frac{f_o}{\dfrac{d(1/(N_{pv} I_r))}{d(1/N_{pv})}} \qquad (6)$$

and

$$k_{rw} = \frac{1 - f_o}{f_o} \frac{\mu_w}{\mu_o} k_{ro} \qquad (7)$$

APPENDIX C

The following Tables give the experimental data obtained from each displacement test. Column 1

gives the cumulative volume of brine in the effluent v_{wc} in pore volumes, column 2 gives the corresponding water saturation as fraction of pore volume and the final column gives the pressure drop across the core in psi.

Table C1.

V_{wc}	S_w	Δp, psi
0.100	0.340	511.60
0.120	0.360	514.80
0.320	0.560	392.70
0.394	0.615	363.20
0.507	0.668	346.50
0.521	0.672	345.20
0.591	0.683	339.90
0.394	0.699	327.50
9.730	0.707	187.20
14.673	0.707	127.60

Core No. B1.
Brine concentration = 15 wt.% NaCl;
Temperature = 15.6°C

Table C2.

V_{wc}	S_w	Δp, psi
0.100	0.410	419.10
0.130	0.440	396.20
0.227	0.509	367.30
0.291	0.541	359.00
0.408	0.578	340.30
0.589	0.612	315.30
1.308	0.659	195.20
2.346	0.671	26.50

Core No. B2.
Brine concentration = 10 wt.% NaCl;
Temperature = 15.6°C

Table C3.

V_{wc}	S_w	Δp, psi
0.100	0.400	434.70
0.120	0.420	411.80
0.237	0.501	373.90
0.301	0.535	363.90
0.602	0.547	334.10
0.654	0.659	326.60
1.103	0.709	256.70
1.798	0.735	145.80

Core No. B3.
Brine concentration = 5% wt.% NaCl;
Temperature = 15.6°C

Table C4.

V_{wc}	S_w	Δp, psi
0.100	0.395	420.50
0.131	0.425	398.10
0.243	0.506	369.50
0.299	0.537	358.00
0.602	0.654	296.50
0.644	0.664	287.30
1.088	0.719	192.10
1.438	0.728	116.60

Core No. B4.
Brine concentration = 0.6 wt.% NaCl;
Temperature = 15.6°C